The design of waveguide filters based on cross-coupled resonators

Shang, Xiaobang; Xia, Wenlin; Lancaster, Michael J.

DOI:
10.1002/mop.27989

Document Version
Publisher's PDF, also known as Version of record

Citation for published version (Harvard):
Shang, X, Xia, W & Lancaster, MJ 2014, 'The design of waveguide filters based on cross-coupled resonators', *Microwave and Optical Technology Letters*, vol. 56, no. 1, pp. 3-8. https://doi.org/10.1002/mop.27989

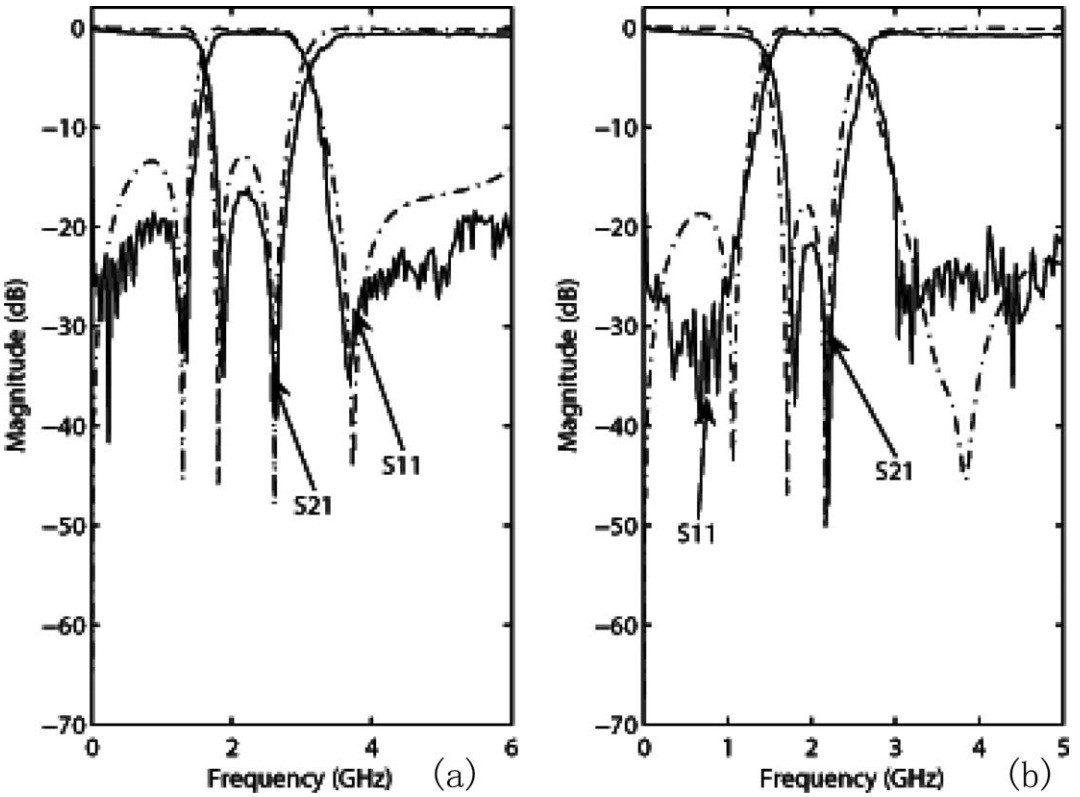

Figure 6 Simulation and measurement performance of the proposed band-stop filters, the solid line is the measurement results, and the dotted line is the simulation results. (a) Band-stop filter using the novel gradually variational stepped impedance hairpin resonator; (b) band-stop filter using the novel gradually variational stepped impedance hairpin resonator with E-shape DGS

4. CONCLUSION

In this article, two novel microstrip band-stop filters using the gradually variational stepped impedance hairpin resonator with DGS or not are presented. By using the gradually variational stepped impedance hairpin resonator, the filters have remarkable advantages, such as compact size, simple structure, and high selectivity. Two band-stop filters are designed, fabricated, and measured. The measurement results show good agreement with the simulation ones.

ACKNOWLEDGMENTS

This work was supported by National Natural Science Foundation of China under Grant 61171051. The authors would like to thank the persons in Agilent Open Laboratory in Beijing, for their technical assistance.

REFERENCES

1. L.H. Hsieh and K. Chang, Compact lowpass filter using stepped impedance hairpin resonator, Electron Lett 37 (2001), 899–900.
2. L.-H. Hsieh and K. Chang, Compact elliptic-function low-pass filters using microstrip stepped-impedance hairpin resonators, IEEE Trans Microwave Theory Tech 51 (2003), 193–199.
3. X.B. Wei, P. Wang, M.Q. Liu, and Y. Shi, Compact wide-stopband lowpass filter using stepped impedance hairpin resonator with radial stubs, Electron Lett 47 (2011), 862–863.
4. L. Li, Z.-F. Li, and J.-F. Mao, Compact lowpass filters with sharp and expanded stopband using stepped impedance hairpin units, IEEE Microwave Wireless Compon Lett 20 (2010), 240–242.
5. K.J. Song, F. Zhang, C.L. Zhuge, and Y. Fan, Compact dual-band band-pass filter using spiral resonators and short-circuited stub-loaded resonator, Microwave Opt Technol Lett 55 (2013), 1393–1398.
6. L. Athukorala, Compact filter configurations using concentric microstrip open-loop resonators, IEEE Microwave Wireless Compon Lett 22 (2012), 245–247.
7. D.S. La, Y.H. Lu, N. Liu, D.N. Cui, J.L. Zhang, New microstrip fractal-shaped square patch resonators filters, Microwave Opt Technol Lett 53 (2011), 1950–1952.
8. J.Q. Lu and D.S. La, Novel band-pass filters using e-shape resonators, J Electromagn Waves Appl 27 (2013), 458–463.
9. D.S. La and Y.H. Lu, Novel band-pass filters using complementary split ring resonators, Microwave Opt Technol Lett 54 (2012), 449–451.

THE DESIGN OF WAVEGUIDE FILTERS BASED ON CROSS-COUPLED RESONATORS

Xiaobang Shang, Wenlin Xia, and Michael J. Lancaster
School of Electronics, Electrical and Computer Engineering, the University of Birmingham, Birmingham, B15 2TT, United Kingdom; Corresponding author: shangxiaobang@gmail.com

Received 17 April 2013

ABSTRACT: *This article addresses the physical realization of cross-coupled waveguide filters based on electromagnetic (EM) simulations. For this design procedure, the filter structure is simulated by successively adding one resonator at a time. The desired filter response is achieved without the need of a global optimisation on all the mechanical dimensions within an EM simulator. This reduces the design time required for a crosscoupled waveguide filter and allows the possibility of building high-order waveguide filters with complex crosscouplings.*

A sixth order X-band dual-band filter with a center frequency of 10 GHz and a fractional bandwidth of 1% is designed using this procedure and presented here as an example. Excellent agreement between simulation results and theoretical results from coupling matrix verifies the proposed approach. © 2014 The Authors. Microwave and Optical Technology Letters Published by Wiley Periodicals, Inc. Microwave Opt Technol Lett 56:3–8, 2014; View this article online at wileyonlinelibrary.com.
DOI 10.1002/mop.27989

Key words: *filter; waveguide; crosscoupling; coupling matrix; dual-band filter*

1. INTRODUCTION

A microwave filter is a two-port network used to transmit and attenuate signals in specified frequency bands. Microwave filters have found wide applications in modern communication systems, radar systems, and laboratory measurement equipments [1]. Filters based on crosscoupled resonators, with real or complex transmission zeros (TZs), have been extensively used to (i) improve the close-to-band selectivity; (ii) achieve in-band group delay linearity; (iii) divide the single-band into multiple passbands. However, compared with the conventional in-line resonator coupled filter, the crosscoupled filter is more difficult to be physically implemented, due to the interactions introduced by the crosscouplings.

Traditionally, the design methods for direct coupled filters have been applied to extract the dimensions for crosscoupled filters. This design process usually involves the following four main steps: (i) identify the filter order and filter functions according to specification requirements; (ii) synthesis or optimise the coupling coefficients ($M_{i,j}$) and external quality factors (Q_e) that can realize the desired filter function; (iii) choose the filter type (waveguide, microstrip, etc), and obtain dimensions which can achieve desired specified Q_e and $M_{i,j}$ from electromagnetic (EM) simulations on one resonator and two weakly coupled resonators; (iv) construct the filter in the simulator to get its initial responses [1, 2]. For crosscoupled filters, this approach ignores the influences from crosscouplings, and therefore normally requires a global optimization on all the physical dimensions. This global optimization is time-consuming, and in some special scenario, where the filter consists of a large number of resonators and/or complex crosscouplings, the final optimization may fail to converge to an acceptable solution, due to the large amount of control parameters. In [3], a design procedure, which eliminates the need of global optimization, has been presented for a crosscoupled folded waveguide filter. A fourth order and a sixth order crosscoupled single-band waveguide filters have been successfully demonstrated using this design approach. However, this design approach is limited to waveguide filters with folded topologies.

In this article, we present an EM-based design approach for determining the physical dimensions of a crosscoupled waveguide filter with any type of topology. This design procedure enables us to account for the attributions of crosscouplings, and provides precise desired dimensions without the need of a final global optimization. This approach may find useful application in the design of resonator based crosscoupled waveguide filters or multiplexers [4].

2. DESIGN STEPS

The design approach is demonstrated by a sixth order X-band dual-band waveguide filter. Figure 1 illustrates the topology and the structure of this filter. This filter is designed to have the following specifications: the center frequency is 9.965 GHz for the first passband and 10.035 GHz for the second passband, both passbands have a desired return loss of 20 dB and the same bandwidth of 30 MHz, the attenuation level for the middle stopband is better than 26 dB. The $N \times N$ coupling matrix of this dual-band filter, as depicted below, is generated by a synthesis technique described in [5]. Their corresponding S-parameter responses can be found in Figure 2. A pair of symmetrical TZs positioned at 9.995 and 10.005 GHz occur at the in-band to split it into two symmetrical passbands. These two TZs are attributed to the crosscoupling between resonators 2 and 5. As all the coupling coefficients are positive, thereby all inductive irises have be utilized by this filter.

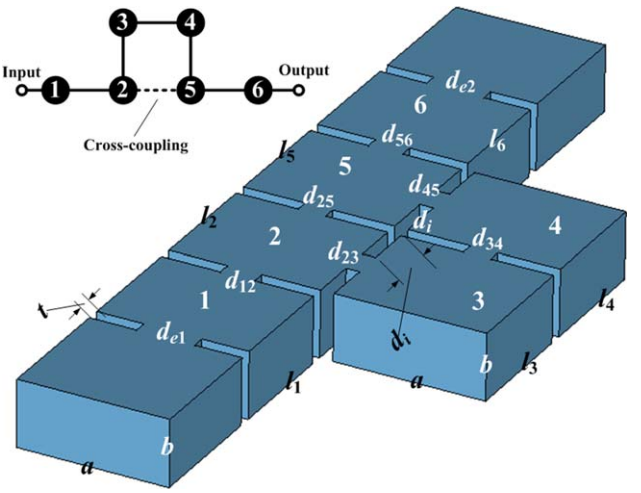

Figure 1 Illustration of a sixth order X-band dual-band waveguide filter and its topology. There is a cross coupling between resonators 2 and 5. These six resonators are operating at TE101 mode and they are coupled together through inductive irises. All the irises have the same thickness t of 2 mm, $a = 22.86$ mm, $b = 10.16$ mm, $di = 5.19$ mm. [Color figure can be viewed in the online issue, which is available at wileyonlinelibrary.com]

$$M = \begin{pmatrix} 0 & 0.00852 & 0 & 0 & 0 & 0 \\ 0.00852 & 0 & 0.00372 & 0 & 0.00388 & 0 \\ 0 & 0.00372 & 0 & 0.00384 & 0 & 0 \\ 0 & 0 & 0.00384 & 0 & 0.00372 & 0 \\ 0 & 0.00388 & 0 & 0.00372 & 0 & 0.00852 \\ 0 & 0 & 0 & 0 & 0.00852 & 0 \end{pmatrix}$$

$$Q_{e1} = Q_{e6} = 145.77.$$

The design can be divided into six substeps, as shown in Figure 3. At work step, rather than optimizing dimensions for the entire structure, only the dimensions of one cavity and its connecting irises are significantly tuned toward the desired responses. This reduces the number of dimensions to be adjusted during the design, which in return yields faster and more reliable convergence. Especially for large scale filter structure, in which case it is virtually impossible to optimize all the mechanical dimensions at the same time. The calculation of the physical dimensions for the sixth order dual-band filter shown in Figure 1 comprises the following steps.

1. Calculate the approximate initial dimensions for all the resonators and irises using the equivalent circuit models based on the coupling matrix as described in [1, 6, 7].

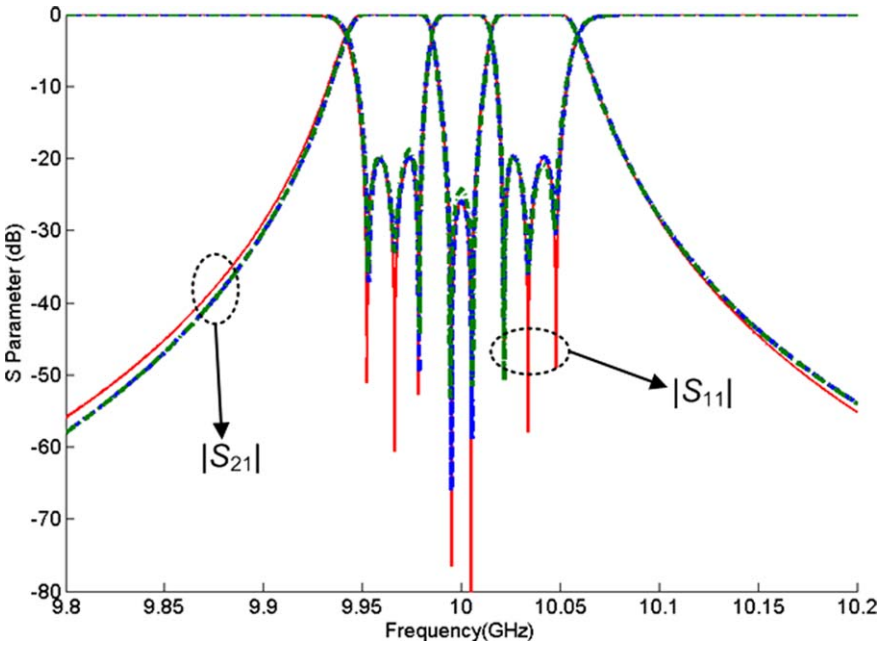

Figure 2 The X-band dual-band filter results from coupling matrix (red solid lines), μwave wizard simulations (dashed blue lines) and CST simulations (dotted green lines). Dimensions obtained at Step 6 shown in Tables 1 and 2 have been used in these simulations. [Color figure can be viewed in the online issue, which is available at wileyonlinelibrary.com]

2. Using the coupling matrix values calculated for the entire filter, obtain just the responses for the first resonator [see Fig. 3(a)]. Use the full-wave simulator (in our case, μwave wizard [8]) to evaluate resonator 1 together with its two adjacent irises, and optimize this simulated response toward the desired one from coupling matrix, by changing the resonator length (l1) and iris dimensions (de1 and d12).
3. Use the EM simulator for both resonators 1 and 2 and their connecting irises [see Fig. 3(b)]. Adjust the length of resonator 2 (l2) and iris dimensions (d23 and d25) to match the responses with the target ones derived from the coupling matrix. The dimensions associated with resonator 1 obtained in Step 2 should be slightly adjusted to account for the influence of resonator 2. This can be done with optimizations and has a fast convergence due to the final result being close to the optimum.
4. Progress through the filter structure by adding only one resonator into the simulated structure at each time, as illustrated

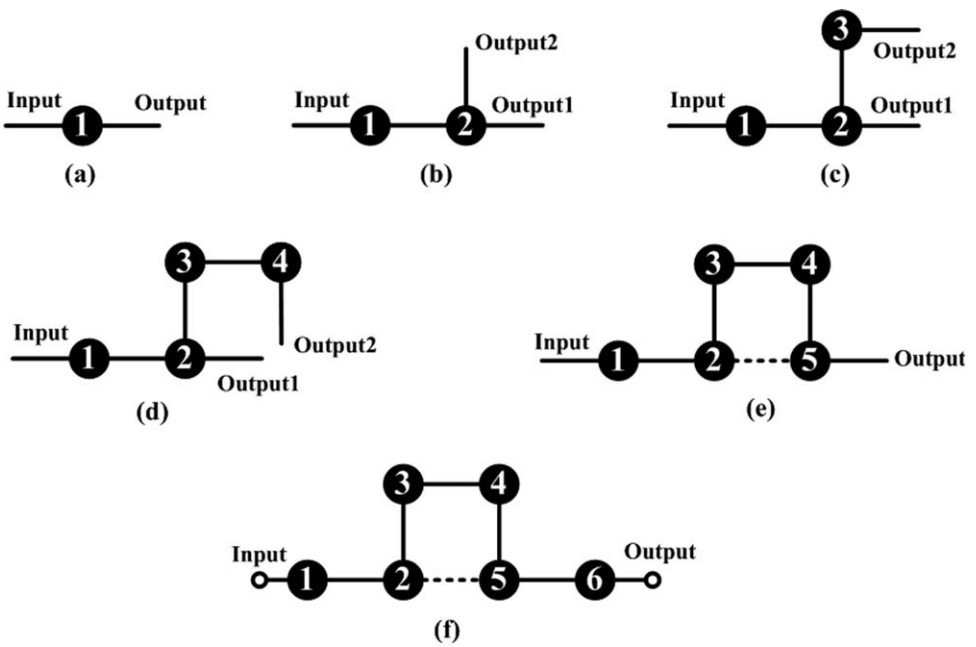

Figure 3 The dual-band filter structure shown in Figure 1 is constructed successively by adding one resonator at a time. The six steps of this design procedure are shown in (a)–(f) in sequence

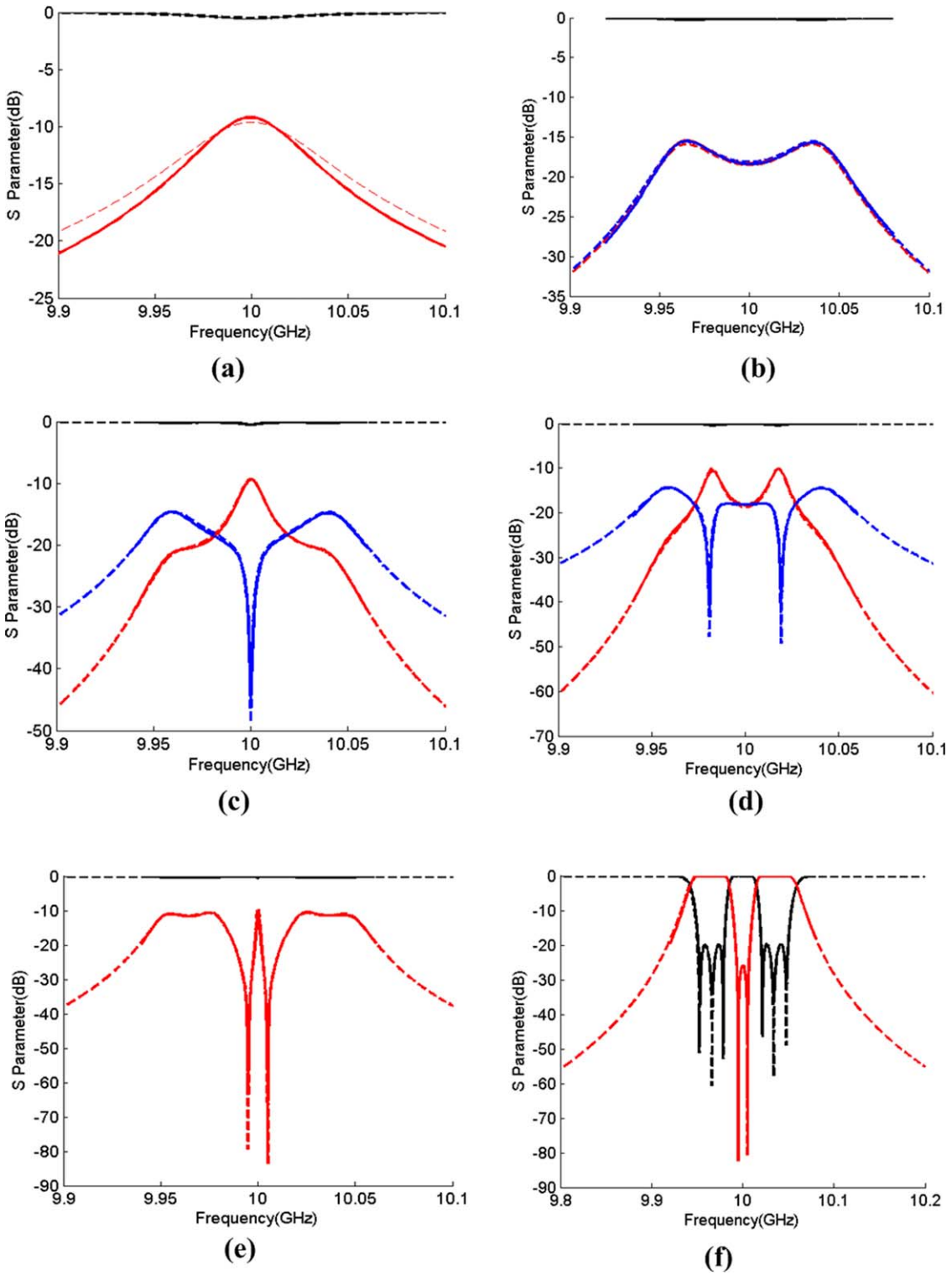

Figure 4 *S*-parameters of the dual-band filter as successive resonators are added and tuned. Their corresponding topologies can be found in Figure 3. Note that, *S*11 responses are included and represented using black lines in all six graphs. The dashed lines represent the desired responses which are plotted from coupling matrix, whereas the solid lines correspond to the responses from simulations using the optimized dimensions given in Tables 2 and 2. [Color figure can be viewed in the online issue, which is available at wileyonlinelibrary.com]

in Figure 3. Optimize the dimensions of the subsequent resonator toward the desired S-parameter responses calculated from coupling matrix. A slight readjustment of the dimensions of the preceding resonators may be required to factor in the influence from the new added resonator. Normally, this small adjustment in dimensions is only required for adjacent resonators. For instance, at the last step [see Fig. 3 (f)], the dimensions of resonator 1 will remain the same as the ones obtained in Step 5, since resonator 6 has a negligible impact on resonator 1.

For this design approach, the middle stage S-parameter responses are calculated from their corresponding coupling coefficients, and act as the objective responses for the tuning. To plot the desired responses at each stage, the inner coupling coefficient needs to be converted into external quality factor. For instance, at Step 1, Q_{e2} should be calculated from M_{12}. After expressing both the external quality factor (Q_e) and internal coupling coefficients (M_{ij}) using inverter value K [1], the relationship between M_{ij} and Q_e can be found as:

$$M_{ij}^2 \cdot Q_e = \frac{1}{\frac{\pi}{2} \cdot \left(\frac{\lambda_g}{\lambda}\right)^2} \tag{1}$$

where λ_g is guided wavelength and λ is the free-space wavelength. For an X-band waveguide filter operating at a center frequency of 10 GHz, $M_{ij}^2 \times Q_e$ is calculated to be 0.3625. Consequently, M_{ij} can be converted to its corresponding Q_e. It is interesting to note that, the value of $M_{ij}^2 \times Q_e$ does not depend on the fractional bandwidth (FBW) of the filter.

In additional, it may be observed from Figure 3 that, for work steps 2 to 5, there are three external ports. However, both equations of $N \times N$ [2] and $(N+2) \times (N+2)$ [1] matrix are derived for a two-port network circuit. In the following, the equations for $(N+3) \times (N+3)$ matrix, which can be applied to calculate S-parameter responses of a three-port filter network, will be derived and given.

Ref. 4 reports equations for computing three-port filter network S-parameter responses. However, these equations are derived following the similar approach to a $N \times N$ coupling matrix [2], and therefore has a restriction that the resonators number should be larger than the number of external ports. In the work presented here, there exists a case that the resonator number is less than the number of ports [see Fig. 3(b)], thereby a similar approach to the $(N+2) \times (N+2)$ matrix synthesis is applied in this work to derive the equations. Here, the relationship between the S-parameters and the coupling matrix is extracted by analyzing the node voltage and current of the three-port network's equivalent circuits, as described in detail in [1, 2, 4]. The matrix m for a general three-port network consists of N coupled resonators, one input port (S) and two output ports ($L1$, $L2$) can be written in the following form:

$$m = \begin{array}{c|cccccccc} & S & 1 & 2 & 3 & \dots & N & L1 & L2 \\ \hline S & & m_{s,1} & m_{s,2} & m_{s,3} & \dots & m_{s,N} & m_{s,L1} & m_{s,L2} \\ 1 & m_{1,s} & m_{1,1} & m_{1,2} & m_{1,3} & \dots & m_{1,N} & m_{1,L1} & m_{1,L2} \\ 2 & m_{2,s} & m_{2,1} & m_{2,2} & m_{2,3} & \dots & m_{2,N} & m_{2,L1} & m_{2,L2} \\ 3 & m_{3,s} & m_{3,1} & m_{3,2} & m_{3,3} & \dots & m_{3,N} & m_{3,L1} & m_{3,L2} \\ \vdots & \vdots & \vdots & \vdots & \vdots & & \vdots & \vdots & \vdots \\ N & m_{N,s} & m_{N,1} & m_{N,2} & m_{N,3} & \dots & m_{N,N} & m_{N,L1} & m_{N,L2} \\ L1 & m_{L1,s} & m_{L1,1} & m_{L1,2} & m_{L1,3} & \dots & m_{L1,N} & & m_{L1,L2} \\ L2 & m_{L2,s} & m_{L2,1} & m_{L2,2} & m_{L2,3} & \dots & m_{L2,N} & m_{L2,L1} & \end{array} \tag{2}$$

The above matrix is symmetrical about the principal diagonal and it includes the couplings between external ports and the internal resonators. Additionally, it is also possible to accommodate the direct couplings between external ports, such as $m_{S,L1}$, $m_{S,L2}$, and $m_{L1,L2}$. The dual-band filter presented here does not include any direct coupling between ports, as shown in Figure 3, therefore $m_{S,L1}$, $m_{S,L2}$. and $m_{L1,L2}$ are assigned to zero here. The highlighted part (using grey colour) represents the core $N \times N$ matrix, whose entries are normalized coupling coefficients ($m_{ij} = M_{ij}$/FBW). The coupling coefficients between external ports and inner resonators can be calculated by

$$m_{S,1} = \frac{1}{\sqrt{q_{e1}}}, \quad m_{N1,L1} = \frac{1}{\sqrt{q_{e2}}}, \quad m_{N2,L2} = \frac{1}{\sqrt{q_{e3}}} \tag{3}$$

where q_{ei} is the normalized external quality factors of the external port i ($q_{ei} = Q_{ei} \times$ FBW), N_1 and N_2 refer to the resonator number connecting to the output ports ($L1$ and $L2$). For instance, at Step 3 as shown in Figure 3(c), $N_1 = 2$, $N_2 = 3$. The general matrix A can be expressed as below

$$[A] = [R] + p[U] - j[m] \tag{4}$$

where U is similar to a $(N+3) \times (N+3)$ unit matrix, except that $U(1,1) = U(N+2,\ N+2) = U(N+3,\ N+3) = 0$, R is a $(N+3) \times (N+3)$ matrix whose only nonzero entries are $R(1,1) = R(N+2,\ N+2) = R(N+3,\ N+3) = 1$, p is the low-pass frequency variable, which can be written in terms of FBW and the filter center frequency (ω_0) as

$$p = j\frac{1}{\text{FBW}}\left(\frac{\omega}{\omega_0} - \frac{\omega_0}{\omega}\right). \tag{5}$$

Then the S-parameter responses of a three-port filter network can be expressed as:

$$\begin{aligned} S_{11} &= 1 - 2[A]_{1,1}^{-1} \\ S_{21} &= 2[A]_{N+2,1}^{-1} \\ S_{31} &= 2[A]_{N+3,1}^{-1} \end{aligned} \tag{6}$$

For the case where there are more than three external ports, similar equations can be derived accordingly by adding extra rows at the bottom and extra columns at the right, to the coupling matrix shown in Eq. (2).

3. RESULTS

The six substep responses for the structures shown in Figure 3 are depicted in Figure 3. In Figure 4, the dashed lines refer to the theoretical responses plotted using the equations described in section 2, and these responses are served as goals of the dimensional tuning. The μwave wizard [8] based on mode-matching technique is used in the simulations. The simulated responses using the optimized dimensions are denoted as solid lines in Figure 4.

At each substep, initially only one resonator's dimensions (three or less parameters) are tuned in the simulations. Therefore, a desired set of dimensions, whose corresponding responses match the objective ones, can be obtained within a short time. The dimensions from the previous stages may also be slightly altered to tune the responses toward the desired ones, as shown in Tables 1 and 2. It can be observed that, only very small adjustments are required on the dimensions achieved in the foregoing stages, to account for the influence from the subsequent resonators.

The final dimensions of the dual-band filter are shown in Tables 1 and 2 (Step 6), and their corresponding simulation results can be found in Figure 2. It can be observed that, without any global optimization, the final acquired dimensions have extremely close responses with the theory ones from coupling matrix. It should be pointed out that, both μwave wizard and

TABLE 1 Dual-Band Filter Iris Dimensions at Each Step

	Dimensions of iris (mm)							
Step	d_{e1}	d_{12}	d_{23}	d_{25}	d_{34}	d_{45}	d_{56}	d_{e2}
1	8.42	5.06	–	–	–	–	–	–
2	8.71	5.17	4.41	4.14	–	–	–	–
3	8.70	5.18	4.65	4.13	4.13	–	–	–
4	8.73	5.15	4.67	4.13	4.14	4.38	–	–
5	8.70	5.17	4.63	4.12	4.13	4.62	5.17	–
6	8.70	5.17	4.63	4.12	4.13	4.62	5.17	8.76

TABLE 2 Dual-Band Filter Resonators Length at Each Step

	Length of resonators (mm)					
Step	l_1	l_2	l_3	l_4	l_5	l_6
1	18.2	–	–	–	–	–
2	18.06	19.01	–	–	–	–
3	18.07	18.99	19.39	–	–	–
4	18.06	18.99	19.39	19.41	–	–
5	18.06	18.99	19.39	19.40	18.99	–
6	18.06	18.99	19.39	19.40	18.98	18.05

CST microwave studio [9] have been used to simulate the dual-band filter. These two EM simulators produce very close results, as shown in Figure 2.

4. CONCLUSION

A mechanical dimensions calculation method for crosscoupled waveguide filters has been described. During this design procedure, the filter structure is constructed step by step by adding one resonator to the simulated structure at a time. Dimensions of this resonator are tuned toward the desired target middle stage responses. Equations have been derived and provided in this article to plot the middle stage responses from coupling matrix. A sixth order dual-band X-band filter with a pair of symmetrical TZs has been successfully demonstrated using this approach. This approach eliminates the need of a global EM-based dimensional optimization, and therefore leads to a reduction in the time required. Moreover, it also opens the possibility of building high-order waveguide filters with complex crosscouplings.

ACKNOWLEDGMENT

This work was supported by the U.K. Engineering and Physical Science Research Council (EPSRC) under contract EP/H029656/1.

REFERENCES

1. R.J. Cameron, C.M. Kudsia, and R.R. Mansour, Microwave filters for commmunication systems, Wiley, Hoboken, NJ, 2007.
2. J.S. Hong and M.J. Lancaster, Micrsotrip filters for RF/microwave applications, Wiley, New York, NY, 2001.
3. J. Kocbach and K. Folgero, Design procedure for waveguide filters with cross-couplings, In: IEEE MTT-S International Microwave Symposium, Seattle, WA, June 2002, pp. 1449–1452.
4. T.F. Skaik, M.J. Lancaster and F. Huang, Synthesis of multiple output coupled rsoantor circuits using coupling matrix optimisation, IET Microwave Antenna Propag 5 (2011), 1081–1088.
5. X. Shang, Y. Wang, G.L. Nicholson, and M.J. Lancaster, Design of multiple-passband filters using coupling matrix optimisation, IET Microwave Antenna Propag 6 (2012), 24–30.
6. F.M. Vanin and D. Schmitt, R. Levy, Dimensional synthesis for wideband waveguide filters, In: IEEE MTT-S International Microwave Symposium, Fort Worth, TX, June 2004, 463–466.
7. F.M. Vanin, D. Schmitt, and R. Levy, Dimensional synthesis for wide-band filters and diplexers, IEEE Trans Microwave Theory Tech 52 (2004), 2488–2495.
8. μwave wizard, Mician GmbH, 2012.
9. CST Microwave Studio Germany, CST GmbH, 2006.

FAST PROTOTYPE-BASED DESIGN APPROACH TO HIGHLY MINIATURIZED LTCC BPFS FOR WLAN/WIMAX DUAL-MODE APPLICATIONS

Hui-Hsiang Huang and Tzyy-Sheng Horng
Department of Electronic Engineering, National Sun Yat-Sen University, No. 70, Liehai Road, Kaohsiung, 80424, Taiwan, Republic of China; Corresponding author: d933010016@student.nsysu.edu.tw

Received 22 April 2013

ABSTRACT: *A novel and fast prototype-based approach is presented to design LTCC band pass filters (BPFs) using two reflection zeros for 2.4 GHz WLAN / 2.3 GHz worldwide interoperability for microwave access dual-mode applications. The proposed approach derives quite compact formulas for synthesizing a filter prototype to meet the specification requirements in the passband insertion loss and stopband attenuation. From real-time prototype simulation prediction, one can efficiently minimize the filter size under various electrical specifications.* © 2014 Wiley Periodicals, Inc. Microwave Opt Technol Lett 56:8–11, 2014; View this article online at wileyonlinelibrary.com. DOI 10.1002/mop.27986

Key words: *LTCC filter; filter prototype; wireless communications service; reflection zeros; worldwide interoperability for microwave access*

1. INTRODUCTION

The most key band pass filters (BPFs), which are microwave devices that are used in wireless communication systems, have a small size, low insertion loss, superior stopband rejection, and high roll-off rate. Therefore, much of the relevant literature is concerned with designs in which high roll-off rate and wide stopband rejection with excellence. Most of the conventional microstrip filters developed to date are based mainly on transmission-line structures [1, 2]. These filters require too much area because each resonator needs quarter- or half-wavelength to get resonance. Some of the novel structures proposed for reducing filter size include stepped impedance resonator [3] and defected ground structure [4]. However, the proposed designs are still not size-competitive with LTCC filters. To maximize device miniaturization, many filters are designed on an LTCC substrate.

LTCC BPFs play an important role because they can provide satisfactory electrical performance with a compact size. However, the unstoppable trend toward smaller mobile terminals continuously demands for smaller LTCC BPFs. The size evolution of LTCC BPFs for 2.4-GHz instruments, scientific, and measurements band applications in the electronic market of mass production is from the early 3225 (3.2×2.5 mm^2), then to 2520 and 2012, and now toward 1608. Every new generation of product reduces the area almost in half when compared to the prior product. Therefore, miniaturization for LTCC BPFs becomes a more and more challenging work.

The previous researches on the miniaturization of LTCC BPFs for wireless communication applications mainly include the second-